Molecular Determinants for Small Maf Protein Control of Platelet Production[▽]

Hozumi Motohashi,[1]* Rie Fujita,[2] Mariko Takayama,[2] Ai Inoue,[2] Fumiki Katsuoka,[2]
Emery H. Bresnick,[3] and Masayuki Yamamoto[2]

*Center for Radioisotope Sciences[1] and Department of Medical Biochemistry,[2] Tohoku University Graduate School of Medicine,
Sendai 980-8575, Japan, and Wisconsin Institute for Medical Research, Paul Carbone Comprehensive Cancer Center,
University of Wisconsin School of Medicine and Public Health, Madison, Wisconsin 53706[3]*

MafG and p45 possess basic region-leucine zipper (bZip) domains and form a heterodimer called NF-E2, a key regulator of megakaryopoiesis. NF-E2 binds to the Maf recognition element (MARE) and activates transcription of many platelet genes. Since the bZip domain, which mediates DNA binding and heterodimerization, is the only functional domain established for MafG, it has been assumed that MafG is required only for p45 binding to MARE and to facilitate p45-mediated transcriptional activation. Analysis of the C-terminal region of MafG, which is distinct from the bZip domain, revealed that this region contains a nuclear matrix-targeting signal. We used a transgenic complementation rescue assay to delineate the function of the MafG C terminus *in vivo*. Transgenic mice expressing a mutant MafG protein lacking the C terminus (MafGΔC) were crossed into a *MafG*-null background. The compound mutant mice displayed severe thrombocytopenia and splenomegaly, which phenocopied *p45*-null mice. The MafG C terminus is essential for proplatelet formation and platelet gene activation but not for p45 binding to MARE. These results demonstrate that the MafG C terminus is required for NF-E2 function and suggest that efficient targeting of NF-E2 to a specific nuclear scaffold is important to achieve high-level activity.

Transcription factor dimerization is often critical to achieve high-affinity DNA binding. A common scenario is that one subunit contains key functional domains that mediate biochemical steps, such as coregulator recruitment, ligand binding, and protein degradation, while the other subunit functions solely to promote dimerization and DNA binding. This mechanism is exemplified by the basic region-helix loop helix (bHLH) proteins MyoD and Mash1, which heterodimerize with the E proteins E12 and E47 (26), the bHLH-Per-Arnt-Sim proteins Hif1α and Ahr, which heterodimerize with Arnt (26), and the bHLH-leucine zipper proteins Myc and Mad, which heterodimerize with Max (10). In addition, the nuclear receptors TR and VDR heterodimerize with RXR (22). In all instances, the individual subunits lack the capacity to bind DNA as monomers or homodimers. In contrast, DNA binding requires heterodimerization with common subunits.

Small Maf proteins, members of the Maf family of transcription factors, contain a characteristic bZip motif and serve as heterodimeric partners for members of another bZip family, the CNC proteins (31). The CNC-small Maf heterodimer binds to a consensus DNA sequence termed the Maf recognition element (MARE). Six members of the CNC protein family possess multiple domains that confer functional diversity. Whereas p45, Nrf1, Nrf2, and Nrf3 are established transcriptional activators, Bach1 and Bach2 are transcriptional repressors. Because these CNC proteins lack intrinsic DNA binding activity, small Maf proteins are obligatory partners of CNC

proteins that endow them with DNA binding activity and therefore competence to regulate transcription. Three small Maf proteins, MafG, MafK, and MafF, resemble each other and are functionally redundant (31). These proteins have a characteristic bZip module, comprised of a leucine zipper and basic region that mediate dimerization and DNA binding, respectively, but other functional domains have not been described. Small Maf proteins are common subunits of heterodimeric transcription factors containing CNC proteins.

The disruption of *small Maf* genes in mice revealed the critical function of small Maf proteins in promotion of platelet production, maintenance of neuronal function, cytoprotection against xenobiotic and oxidative stress, and negative regulation of the *Ho-1* gene (18, 19, 32, 37, 44). *p45*-null mice exhibit defective platelet production (45), suggesting that the p45-small Maf heterodimer is necessary for the production of platelets from megakaryocytes. The neuron-specific *Nrf1* knockout mice yield neurological disorders (F. Katsuoka and M. Yamamoto, unpublished observation), suggesting that the Nrf1-small Maf heterodimer is necessary for the maintenance of neuronal homeostasis. Cytoprotection against xenobiotic and oxidative stress is impaired in *Nrf2*-null mice (15, 16), suggesting that the Nrf2-small Maf heterodimer mediates the stress response. *Ho-1* gene expression is aberrantly derepressed in *Bach1*-null mice (47), indicating that the Bach1-small Maf heterodimer confers *Ho-1* repression. These phenotypes of small Maf mutant mice are assumed to result from functional deficiencies of heterodimerizing CNC proteins, consistent with the notion that small Maf proteins are requisite partners for CNC proteins. Thus, the only established function of small Maf proteins is conferring binding of CNC proteins to MAREs through the bZip motif.

* Corresponding author. Mailing address: Center for Radioisotope Sciences, Tohoku University Graduate School of Medicine, 2-1 Seiryo-cho, Aoba-ku, Sendai 980-8575, Japan. Phone: 81-22-717-8087. Fax: 81-22-717-8090. E-mail: hozumim@med.tohoku.ac.jp.

Megakaryocytes provide a powerful experimental system to dissect mechanisms underlying the structure/function of small Maf proteins (30). Genetic evidence indicates that the p45-small Maf heterodimer, NF-E2, is required for megakaryocyte proliferation (25, 34), cytoplasmic maturation (45), proplatelet formation (24, 37), and platelet gene expression (2, 6, 34, 48). Since there are three functionally redundant small Maf proteins, most tissues and cell lineages display little or no defects upon deleting a single gene encoding small Maf proteins (36, 44). However, megakaryocytes differ in this regard. Deletion of the *MafG* gene dramatically impairs proplatelet formation and alters the gene expression profile in megakaryocytes (30, 37), suggesting that MafG is critically required for NF-E2 activity in megakaryocytes. Defective NF-E2 activity in *MafG*-null megakaryocytes is restored when MafG or MafK is exogenously expressed from a transgene driven by the *Gata1* hematopoietic regulatory domain (*G1HRD*), which is active specifically in erythroid cells and megakaryocytes *in vivo* (30). Based on this result, we tested a sumoylation-defective MafG mutant, MafG K14R, by generating transgenic mouse lines expressing MafG K14R (33). The transgene-expressed mutant rescued defective NF-E2 activity in *MafG*-null megakaryocytes, and we concluded that MafG sumoylation is not essential for NF-E2 activity in normal megakaryocytes.

To determine if small Maf proteins contain previously undescribed functionally important sequences, we examined amino acid sequences external to the bZip domain. We identified a region of high sequence conservation within the divergent C-terminal region and assessed the functional significance of this region *in vivo*. A MafG mutant lacking this region (MafGΔC) was analyzed in the transgenic complementation rescue system. We generated transgenic mice expressing MafGΔC under the regulation of *G1HRD*, which were crossed into the *MafG*-null background. $MafG^{-/-}$::*G1HRD*-MafGΔC mice resembled *p45*-null mice in displaying defective megakaryopoiesis. Since p45 occupied MAREs in the target genes even in $MafG^{-/-}$::*G1HRD*-MafGΔC megakaryocytes, the C-terminal region exerts a critical function to confer NF-E2 transcriptional activation independently of DNA binding. Since the MafG C terminus contains a nuclear matrix-targeting sequence, it is attractive to propose that this sequence ensures a specific subnuclear localization required for the control of megakaryopoiesis.

MATERIALS AND METHODS

Plasmids. pIM-His-MafG XB and pIM-His-MafGΔC XB were used as expression vectors for MafG and MafGΔC. pIM-His-MafG XB was described previously (33). pIM-His-MafGΔC XB was generated by inserting the XbaI-BamHI fragment of pET15b-MafG1-123 (23) into the NotI-NotI fragment of pIM-LacZ (29). pRBGP2, a reporter plasmid carrying the firefly luciferase gene driven by triplicate MAREs, and pEF-p45, a p45 expression vector, were previously described (14). To construct an expression vector for a fusion protein combining enhanced yellow fluorescent protein with nuclear localization signals (EYFP-Nuc) and the MafG C terminus, a DNA fragment encoding MafG124-162 was amplified by PCR and cloned into pGEM-T (Promega). The NcoI-PstI fragment of the plasmid was inserted into the BamHI site of pEYFP-Nuc (Clontech) to generate pEYFP-Nuc-GCR.

Transient transfection and reporter assay. 293T cells were maintained in Dulbecco's modified Eagle medium (DMEM) (Sigma) containing 10% fetal bovine serum, 50 U/ml penicillin, and 50 μg/ml streptomycin. pRBGP2 was introduced into 293T cells along with the pEF-p45 p45 expression vector and the MafG or MafGΔC expression vector pIM-His-MafG XB or pIM-His-MafGΔC

XB, respectively, using the FuGENE6 transfection reagent (Roche) according to the manufacturer's protocol. Cells were harvested at 24 h after transfection. For Western blotting, cells were lysed in 1× SDS gel loading buffer (50 mM Tris-HCl, pH 6.8, 100 mM dithiothreitol [DTT], 2% SDS, and 10% glycerol). Western blotting was performed with anti-p45 antibody (sc-291; Santa Cruz) and anti-His antibody (sc-804; Santa Cruz). For the reporter assay, cells were lysed in passive lysis buffer (Promega). The expression levels of both firefly and sea pansy luciferase were quantified using the dual-luciferase reporter assay system (Promega) and a luminometer (Berthold Japan, Tokyo, Japan). Firefly luciferase activity was normalized to the level of activity for cotransfected sea pansy luciferase to quantify the transfection efficiency. All samples were prepared in triplicate, and averages and standard deviations were calculated.

EMSA. An electrophoretic mobility shift assay (EMSA) was performed as described previously (33). To produce full-length MafG and MafGΔC in *Escherichia coli*, pET15b-MafG(1-162) and pET15b-MafG(1-123) were introduced into *E. coli* BL21(DE3), respectively. To produce p45ΔN encompassing the CNC and bZip motifs of p45, pET15b-p45(221-360) was generated by inserting the DNA fragment encoding p45 polypeptide (amino acids [aa] 221 to 360) into pET15b (Novagen) and similarly introduced into *E. coli* BL21(DE3). The bacterial lysates were incubated with Probond resin (Invitrogen) at 4°C for 1 h. The associated proteins were eluted with 500 mM imidazole and dialyzed against the phosphate buffer (20 mM sodium phosphate [pH 7.8], 10% glycerol, 200 mM NaCl, 1 mM DTT, and 1 mM phenylmethylsulfonyl fluoride [PMSF]). A double-stranded DNA probe containing an NF-E2 binding site from the human porphobilinogen deaminase (*PBGD*) promoter was prepared by annealing 5'-TGG GGA ACC TGT GCT GAG TCA CTG GAG-3' to 5'-CCT CCA GTG ACT CAG CAC AGG TTC CCC-3' and radiolabeled with [γ-^{32}P]ATP. The protein-DNA complexes and free probe were resolved by electrophoresis on a 5% polyacrylamide (79:1) gel in 1× Tris-borate-EDTA (TBE) buffer.

Nuclear matrix association. 293T cells were transfected with pEYFP-Nuc or pEYFP-Nuc-GCR and harvested after 24 h. *In situ* nuclear matrix isolation was conducted as described previously (7, 39). Briefly, transfected cells were directly extracted with CSK buffer on a chamber slide (10 mM piperazine-*N-N'*-bis(2-ethanesulfonic acid) (PIPES) [pH 6.8], 100 mM KCl, 300 mM sucrose, 3 mM MgCl₂, 1 mM EGTA, 0.5% Triton X-100, and 1.2 mM PMSF). After 5 min at 4°C, the cells were incubated with 0.1 mg/ml DNase I in CSK buffer without Triton X-100 for 20 min at 25°C. The cells were extracted with 0.25 M ammonium sulfate in CSK buffer for 5 min at 4°C, washed in phosphate-buffered saline (PBS) containing 1 μg/ml 4',6-diamidino-2-phenylindole (DAPI), and analyzed by fluorescence microscopy. Cell fractionation was conducted under the same conditions. After DNase I treatment and ammonium sulfate extraction, soluble fractions were saved for Western blotting; the insoluble fraction was lysed in 1× SDS sample buffer and considered the nuclear matrix fraction. To prepare cytoplasmic, nuclear, and nuclear matrix fractions, cells were lysed in hypotonic buffer containing 10 mM HEPES (pH 7.9), 1.5 mM MgCl₂, 10 mM KCl, 0.5 mM DTT, 1 mM PMSF, and 1× Complete (Roche) solution. The supernatant was collected as a cytoplasmic fraction. The pellet was sonicated in the hypertonic buffer containing 20 mM HEPES (pH 7.6), 20% glycerol, 400 mM NaCl, 1.5 mM MgCl₂, 0.2 mM EDTA, 1 mM DTT, 1 mM PMSF, and 1× Complete (Roche) solution on ice (level 3, 50% duty, 5 strokes by UltraS Homogenizer VP-15S; Taitec). After a 1-h extraction at 4°C, the supernatant was collected as a nuclear fraction. The insoluble pellet was lysed in 1× SDS sample buffer as a nuclear matrix fraction. Anti-MafG (33), anti-green fluorescent protein (GFP) (sc-8334; Santa Cruz), anti-lamin B (sc-6217; Santa Cruz), antiactin (sc-1615; Santa Cruz), and antitubulin (DH1A; Sigma) antibodies were used in Western blotting.

Mice. Together with control wild-type littermates, *MafG*-null and *p45*-null mice were obtained from *MafG* heterozygous mating pairs (44) and *p45* heterozygous mating pairs (45), respectively. The PCR conditions and primers for genotype determination have been described previously.

Generation of transgenic mice. The generation of *G1HRD*-His-MafG transgenic mice was previously described (33). To construct *G1HRD*-His-MafGΔC, six histidine residues were inserted between the first methionine and the second threonine residues of MafG. The resultant coding sequence was ligated to the *G1HRD* vector. The PCR primers for identification of *G1HRD*-His-MafG are IEint (5'-TGT CTC ACA ACC CTT TCT GTC C-3') and His-MafG1-162 (3'; 5'-CCC TAT GAC CGA GCA TCC GTC TT-3'), and those for identification of *G1HRD*-His-MafGΔC are IEint and His-MafG1-123 3' (5'-AAC TAG CGG GCC ACG GTC CTG GCA AA-3'). Each *G1HRD* construct was coinjected with *G1HRD*-GFP (30). To obtain $MafG^{-/-}$::*G1HRD*-His-MafG and $MafG^{-/-}$::*G1HRD*-His-MafGΔC mice, homozygous *MafG* mutant mice were crossed with *G1HRD*-His-MafG and *G1HRD*-His-MafGΔC transgenic mice, respectively. $MafG^{+/-}$::*G1HRD*-His-MafG or $MafG^{+/-}$::*G1HRD*-His-MafGΔC

mice were crossed with *MafG* homozygous mutant mice, and the resultant litters were used for analysis.

Western blotting. Whole-cell extracts were prepared from transfected 293T cells and bone marrow cells of 4- to 12-week-old mice from each line of transgenic mice. Cytoplasmic and nuclear proteins were isolated from the cells treated with a lysis buffer (20 mM HEPES [pH 7.6], 20% glycerol, 10 mM NaCl, 1.5 mM MgCl$_2$, 0.2 mM EDTA, 1 mM DTT, 1 mM PMSF, 1× Complete [Roche]). Triton X-100 (0.1%) was added in the case of 293T cells. After centrifugation, the supernatant was collected as a cytoplasmic fraction, and the pellet was boiled in SDS sample buffer to yield a nuclear fraction. MafG and MafGΔC were detected using an anti-MafG antibody (33) in the case of bone marrow cells and using an anti-His antibody (sc-804; Santa Cruz) in the case of 293T cells. p45 was detected using an anti-p45 antibody (sc-291; Santa Cruz). YFP-Nuc and YFP-Nuc-GCR were detected using an anti-GFP antibody (sc-8334; Santa Cruz). As loading controls, antibodies against lamin B (sc-6217; Santa Cruz) and actin (sc-1615; Santa Cruz) were used.

Hematologic analysis. Whole blood was collected from the retro-orbital sinuses of anesthetized mice, and the red cell counts and platelet counts were determined using an automatic blood cell analyzer (Nihon Koden, Tokyo, Japan).

Histological analysis. Spleens were fixed in 3.7% formalin in PBS. The samples were embedded in paraffin and stained with hematoxylin and eosin (HE) and silver impregnation. Microscopic images were captured with a DP70 digital camera system (Olympus, Tokyo, Japan).

PPF assay. Megakaryocytes were isolated from the bone marrow of 1- to 4-month-old mice; the projection of proplatelets was observed as described previously (37). Only GFP-positive cells were counted for the calculation of the proplatelet formation (PPF) ratios, except for counts in wild-type and *MafG*-null mice.

Purification of bone marrow megakaryocytes. CD41-positive cells were isolated from bone marrow by the MACS cell separation system (Miltenyi Biotec). Bone marrow cells were collected as described previously (37), reacted with fluorescein isothiocyanate (FITC)-labeled anti-mouse CD41 antibody (Pharmingen), and mixed with anti-FITC microbeads (Miltenyi Biotec). The associated cells were separated using a large cell separation column (Miltenyi Biotec). For RNA purification, CD41-positive cells were pooled from three independent animals from each line.

Primary megakaryocyte culture. Whole livers were recovered from mouse fetuses at embryonic day 14.5 (E14.5), and single-cell suspensions were prepared by successive passage through 25-gauge needles. Fetal liver cells were maintained in RPMI 1640 (Wako) supplemented with 20% charcoal-stripped fetal bovine serum, 50 U/ml penicillin, 50 μg/ml streptomycin, and 50 ng/ml of recombinant human thrombopoietin (TPO) (generously provided by Kyowa Hakko Kirin Co., Ltd., Tokyo, Japan). On the third day of culture, CD41-positive cells were selected using biotinylated anti-CD41 antibody (Serotec) and streptavidin-conjugated Dynabeads (Dynal). CD-41-positive cells were used for RNA purification or chromatin immunoprecipitation assay.

RNA purification and real-time PCR. Total RNA was extracted from the megakaryocytes using the Isogen reagent (Nippon Gene, Tokyo) and reverse transcribed by using Superscript II reverse transcriptase (Invitrogen). Relative mRNA expression levels were quantified using real-time PCR (ABI Prism 7300 sequence detection System). The probes and primers for detecting *Txas*, *Slc6a4*, *Slamf1*, *Selp*, *Gp6*, and *Nqo1* have been described previously (34).

ChIP assays. Chromatin immunoprecipitation (ChIP) assays were performed as previously described (21) using 3-day primary cultures of megakaryocytes from E14.5 fetal livers. Immunoprecipitation was performed using control rabbit IgG, anti-p45 (28), anti-trimethyl-histone H3 (K4) (Upstate 07-473), and anti-acetyl histone H3 (Upstate 06-599) antibodies. The primers and probe used for amplifying the *Txas* promoter, *Nqo1* promoter, and *Txas* intron were described previously (34). Relative enrichment compared to the input was calculated after the immunoprecipitation.

RESULTS

Identification of a highly conserved sequence within the C termini of small Maf proteins. To investigate whether small Maf proteins contain previously undescribed regulatory sequences, we aligned amino acid sequences of small Maf proteins from various vertebrates (Fig. 1A). The core structures of Maf proteins, including the basic region, leucine zipper (bZip) motifs, and extended homology regions (EHR), are highly conserved among all small Maf proteins: MafG, MafK, MafF, and MafT. Outside the core structures, well-conserved sumoylation consensus motifs reside in the N-terminal regions (33). The C-terminal regions, which are more diverse than the N-terminal regions, contain a stretch of eight amino acids that is completely conserved among all small Maf proteins (SVITIVKS). The N-terminal flanking portion of the stretch is also well conserved between MafG and MafK. Our previous study showed that MafG and MafK are interchangeable in rescuing defects in *MafG*-null megakaryocytes (30), suggesting that the distinct portions between MafG and MafK are not essential and that the common portions between MafG and MafK are important for their function in megakaryocytes. Although the C-terminal region is dispensable with regard to DNA binding *in vitro* (as either a homodimer or a heterodimer with CNC proteins) (33, 49), the presence of highly conserved sequences within the C-terminal region prompted us to investigate the contribution of this region to small Maf protein function *in vivo*.

We generated MafGΔC by deleting 39 amino acids from the C terminus and compared the function of MafGΔC to that of full-length MafG. The DNA binding capacities of MafG and MafGΔC were compared by EMSA (Fig. 1B). Bacterially expressed MafG, MafGΔC, and the C-terminal fragment of p45 encompassing the CNC and bZip motifs were purified. MafG or MafGΔC was incubated with p45 and a radiolabeled probe containing the NF-E2 binding site. In the absence of MafG or MafGΔC, p45 did not bind to the probe. Similar amounts of MafG and MafGΔC estimated by Coomassie staining yielded shifted bands of similar intensities in EMSA. Consistent with previous reports (33, 49), the DNA binding activity of the p45-MafG heterodimer *in vitro* was unaffected by the deletion of the C terminus of MafG.

MafG and MafGΔC were transiently overexpressed in 293T cells. Both proteins were detected exclusively in the nuclear fraction (Fig. 1C), indicating that the C terminus is not required for MafG nuclear localization. When the same amount of the MafG or MafGΔC expression vector was introduced into 293T cells with the p45 expression vector and pRBGP2, a MARE-dependent luciferase reporter gene, activation of the reporter gene was stronger at a lower dose and weaker at a higher dose of MafG or MafGΔC expression vectors (Fig. 1D). Importantly, the levels of MafG and MafGΔC expression at each plasmid concentration were similar (Fig. 1E). Previous studies demonstrated that small Maf expressed at a low level heterodimerizes with p45 to activate transcription, whereas at a higher level, small Maf homodimerizes and represses transcription (30, 35). No difference in this regard was detected between MafG and MafGΔC in a reporter assay.

The MafG C terminus contains a nuclear matrix-targeting signal. We examined whether the specific region contains a nuclear matrix-targeting signal, because we observed that small Maf proteins are detected in the nuclear matrix fraction in a biochemical analysis (data not shown). The nuclear matrix, originally defined as an insoluble fraction of nuclei, is believed to constitute a functional scaffold that facilitates nuclear processes, including transcription, splicing, and DNA replication and repair (1, 12, 42, 50).

To examine whether the MafG C terminus has the capacity to target a heterologous protein to the nuclear matrix, we
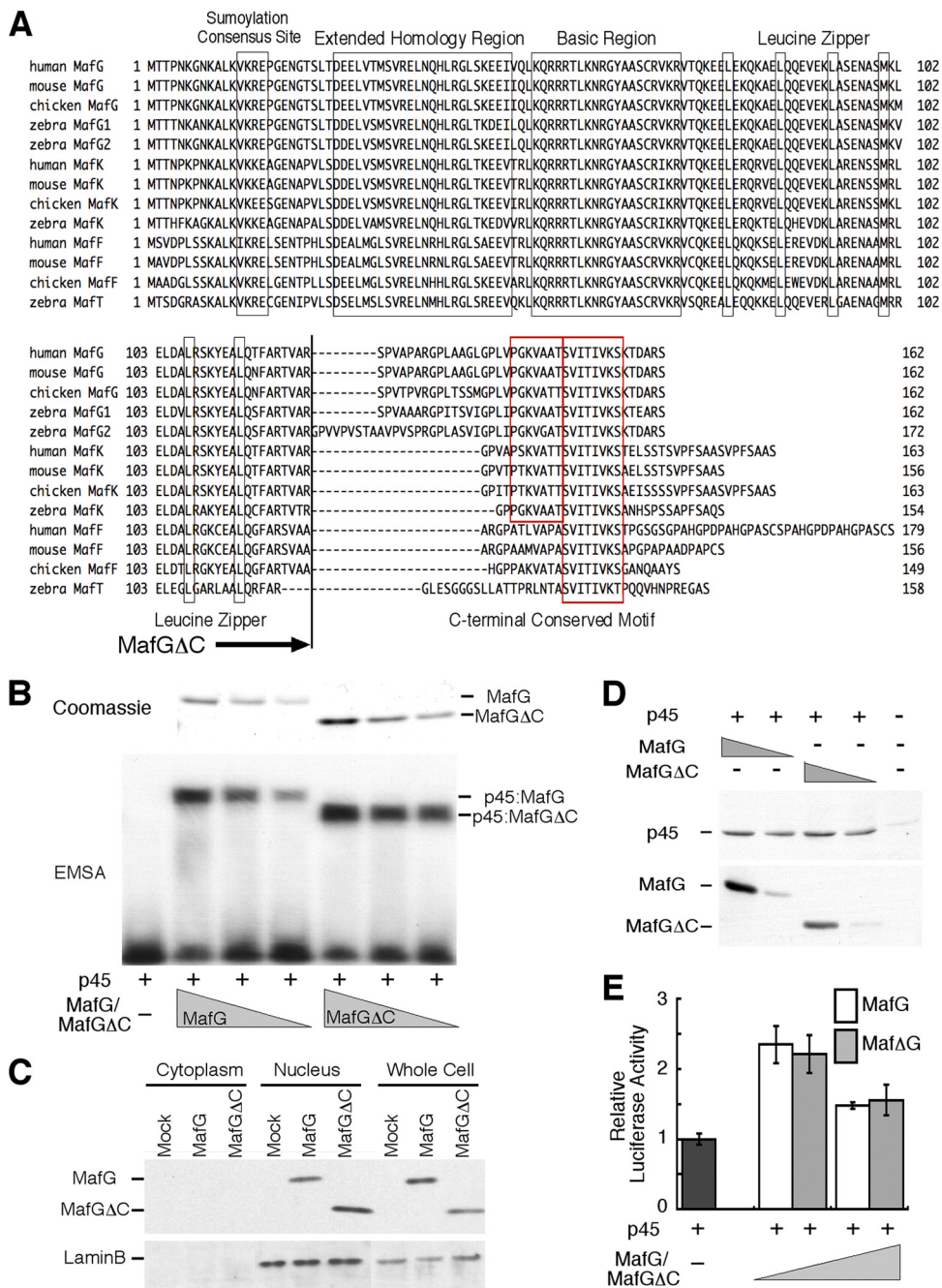
FIG. 1. A highly conserved motif in the diverse C-terminal region of small Maf proteins. (A) Alignment of small Maf proteins of various species. Conserved motifs are boxed. The truncation point of MafGΔC is indicated with an arrow. (B) EMSA of MafG or MafGΔC heterodimerized with p45. Bacterially expressed MafG and MafGΔC used in EMSA were visualized by Coomassie staining (upper panel). Decreasing amounts of MafG and MafGΔC were mixed with a constant amount of the C-terminal half of p45 containing the CNC domain and bZip motif. A 1/40 portion of the protein loaded on each lane of the SDS-PAGE gel was used for the binding reaction in EMSA shown below. The DNA binding capacities of the heterodimers were measured by EMSA (lower panel). The promoter sequence of the human *PBGD* gene containing the NF-E2 binding site was used as a probe. (C) Subcellular localization of MafG and MafGΔC. Cytoplasmic and nuclear fractions were prepared from 293T cells transfected with the expression vector of His-tagged MafG or MafGΔC. MafG and MafGΔC were detected using anti-His antibody. Lamin B and actin were detected as loading controls. (D) Contribution of MafG and MafGΔC to MARE-dependent transcription. The luciferase activity of the sample without MafG or MafGΔC is set to 1. Error bars indicate standard deviations of triplicate samples. (E) Comparison of accumulation of MafG and MafGΔC produced from equivalent amounts of expression plasmids. Both MafG and MafGΔC are tagged with a His tag, and anti-His antibody was used for detection. The transfection efficiency was monitored by determining the abundance of p45 that was coexpressed with MafG or MafGΔC.
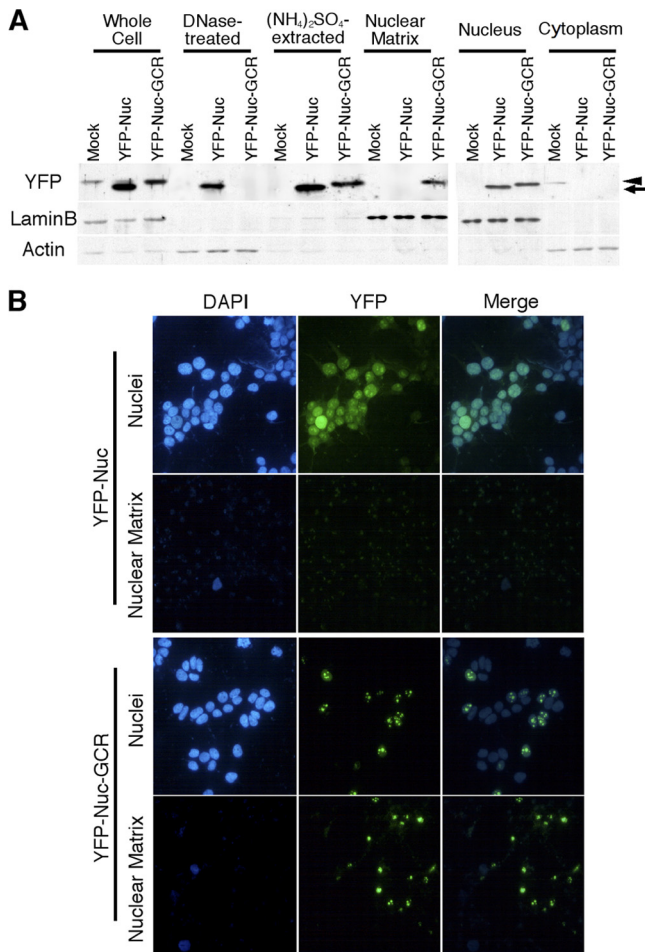
FIG. 2. Nuclear matrix-targeting activity of the MafG C terminus. (A) Cell fractionation was performed using 293T cells transfected with the EYFP-Nuc or EYFP-Nuc-GCR expression vector. EYFP-Nuc and EYFP-Nuc-GCR were detected by anti-GFP antibody. Lamin B and actin were detected as loading controls. An arrow and an arrowhead indicate the band of YFP-Nuc and that of YFP-Nuc-GCR, respectively. (B) *In situ* isolation of nuclear matrix. 293T cells were transfected with the EYFP-Nuc or EYFP-Nuc-GCR expression vector. Upper and lower panels of each construct show cells that were left untreated or treated with sequential extraction.

FIG. 3. Generation of *G1HRD*-MafG and *G1HRD*-MafGΔC mice. Whole-cell extracts from bone marrow of *G1HRD*-MafG and *G1HRD*-MafGΔC mice on the wild-type background (A) or *MafG*-null background (B) were analyzed by Western blotting. Coomassie staining is shown as a loading control. White arrowheads indicate endogenous MafG. Gray and black arrowheads indicate transgene-derived His-tagged MafG and His-tagged MafGΔC, respectively. (C) Cell fractionation was performed using bone marrow cells from *MafG*$^{-/-}$::*G1HRD*-MafG (line 8) and *MafG*$^{-/-}$::*G1HRD*-MafGΔC (line 36) mice. Gray and black arrowheads indicate MafG and MafGΔC, respectively, as detected by anti-MafG antibody. An arrow indicates lamin B. Coomassie staining is shown as a loading control for each fraction.

generated YFP-Nuc-GCR by connecting the MafG C terminus to YFP-Nuc (YFP with nuclear localization signals). YFP-Nuc and YFP-Nuc-GCR were transiently expressed in 293T cells. Fractionation of 293T cells expressing YFP-Nuc or YFP-Nuc-GCR was performed, and YFP-Nuc and YFP-Nuc-GCR were detected by Western blotting using anti-GFP antibody that reacts with YFP (Fig. 2A). Both YFP-Nuc and YFP-Nuc-GCR were detected in the nuclear fraction. YFP-Nuc was almost completely solubilized by DNase treatment and subsequent high-salt extraction, with only a minor portion remaining in the nuclear matrix fraction. YFP-Nuc-GCR was partially solubilized by high-salt extraction, but a substantial portion remained in the nuclear matrix fraction. When 293T cells expressing YFP-Nuc or YFP-Nuc-GCR were morphologically examined after *in situ* extraction, YFP-Nuc-GCR fluorescence was still observed in the nuclear matrix, but that of YFP-Nuc was not
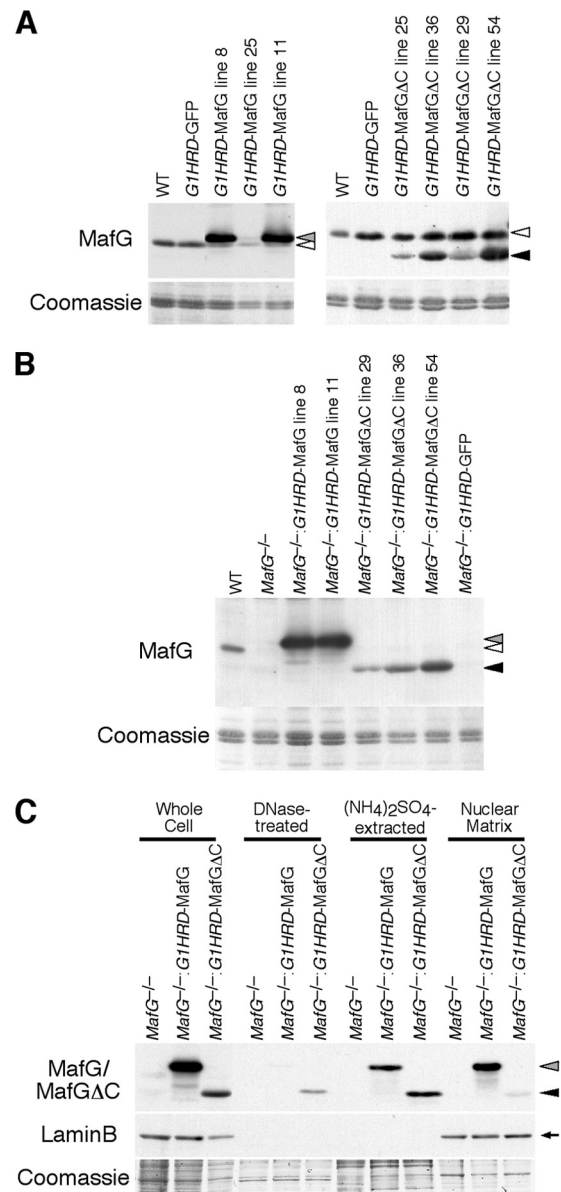
(Fig. 2B). Thus, the MafG C-terminal region contains a nuclear matrix-targeting signal.

Generation of MafGΔC-expressing transgenic mice. To examine the contribution of the MafG C terminus under physiological conditions, we performed transgenic complementation rescue experiments (30). We generated transgenic mice
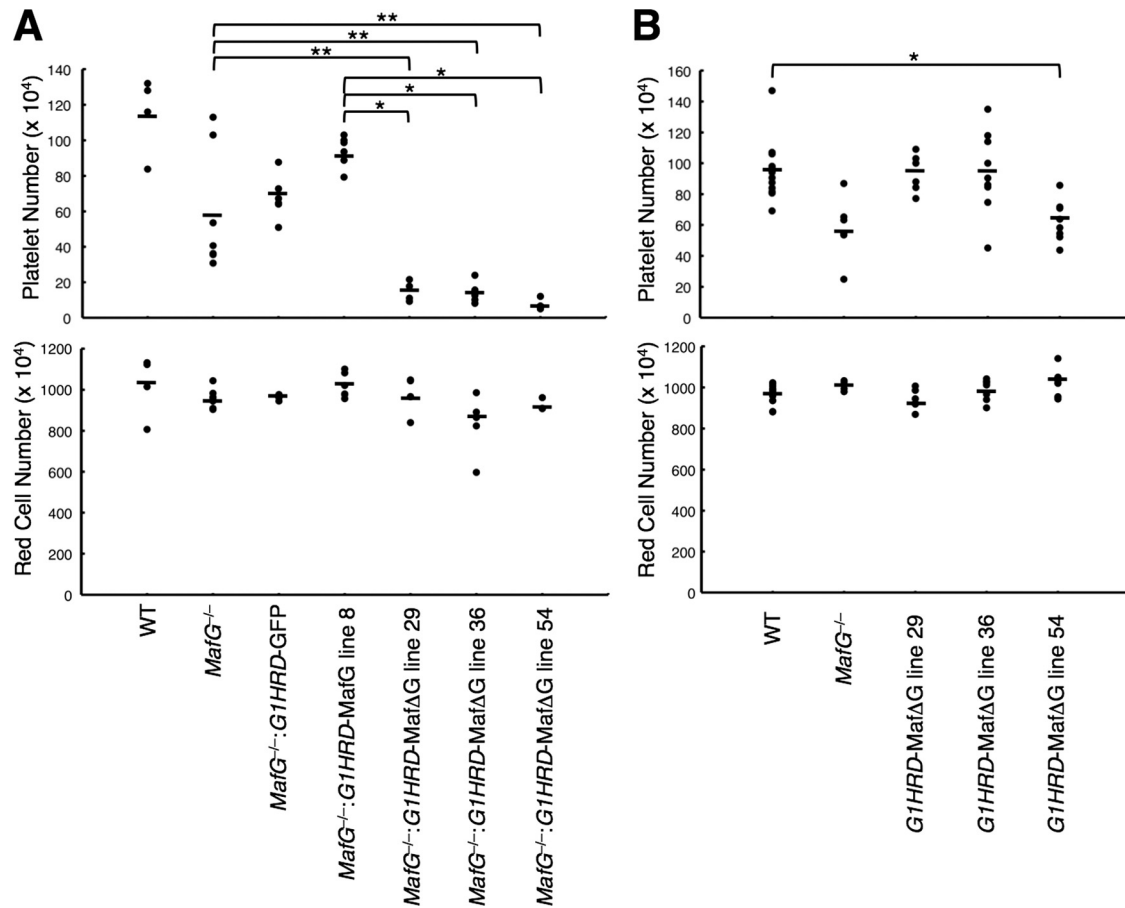
FIG. 4. Hematological parameters of *MafG*^−/−^::*G1HRD*-MafGΔC mice (A) or *G1HRD*-MafGΔC mice (B). Platelet number (upper panels) and red cell number (lower panels) were analyzed using an automated hemocytometer. Each dot indicates the count of an individual animal, and a bar indicates the average value of each mouse line. Student's *t* test was used to calculate statistical significance (*P*). ∗ and ∗∗, *P* < 0.001 and *P* < 0.05, respectively.

expressing MafGΔC under the regulation of *G1HRD*, which is active in erythroid and megakaryocytic cell lineages. A DNA fragment encoding GFP fused to *G1HRD* was coinjected to mark the cells expressing MafGΔC. Four independent lines harboring the *G1HRD*-MafGΔC transgene were established. MafGΔC protein expression by the transgene was examined in Western blotting of bone marrow cells (Fig. 3A). MafGΔC was expressed at a level resembling that of endogenous MafG in line 36, whereas lines 25/29 and 54 showed lower and higher expression, respectively. All mice were fertile and were born in litters conforming to the Mendelian ratio. Transgenic mice expressing full-length MafG (lines 8, 11, and 25) or GFP under the same regulatory cassette were generated in our previous studies (30, 33).

Three lines (lines 29, 36, and 54) of *G1HRD*-MafGΔC mice were crossed with *MafG*-null mice, and *MafG*^+/−^ mice carrying the transgene were obtained. *MafG*^+/−^::*G1HRD*-MafGΔC mice were further crossed with *MafG*-null mice, and *MafG*^−/−^::*G1HRD*-MafGΔC mice were generated. *G1HRD*-MafG mice and *G1HRD*-GFP mice were similarly crossed into the *MafG*-null background. Expression of transgene-derived MafG or MafGΔC in the *MafG*-null background was measured in bone marrow cells by Western blotting (Fig. 3B). The trans-

gene expression levels were unaffected by the presence or absence of endogenous MafG.

Transient overexpression analysis suggested that MafG is anchored to the nuclear matrix through the C-terminal region (Fig. 2). We examined the association of MafG and MafGΔC with the nuclear matrix in *MafG*^−/−^::*G1HRD*-MafG mice and *MafG*^−/−^::*G1HRD*-MafGΔC mice, respectively. Fractionation of bone marrow cells of *MafG*^−/−^::*G1HRD*-MafG and *MafG*^−/−^::*G1HRD*-MafGΔC mice was performed, and MafG and MafGΔC were measured by Western blotting (Fig. 3C). MafG was partially solubilized by high-salt extraction, but a substantial amount persisted in the nuclear matrix. In contrast, the majority of MafGΔC was solubilized by DNase treatment, followed by high-salt extraction. These results indicate that the MafG C terminus mediates MafG association with the nuclear matrix, consistent with the notion that the MafG C terminus contains a nuclear matrix-targeting signal.

MafGΔC exerts dominant-negative activity and does not rescue defects in *MafG*-null megakaryocytes. Hematological phenotypes of the compound mutant mice were examined. Surprisingly, the platelet count was dramatically reduced in *MafG*^−/−^::*G1HRD*-MafGΔC mice, to levels much lower than those of *MafG*-null mice (Fig. 4A, upper panel). MafG defi-
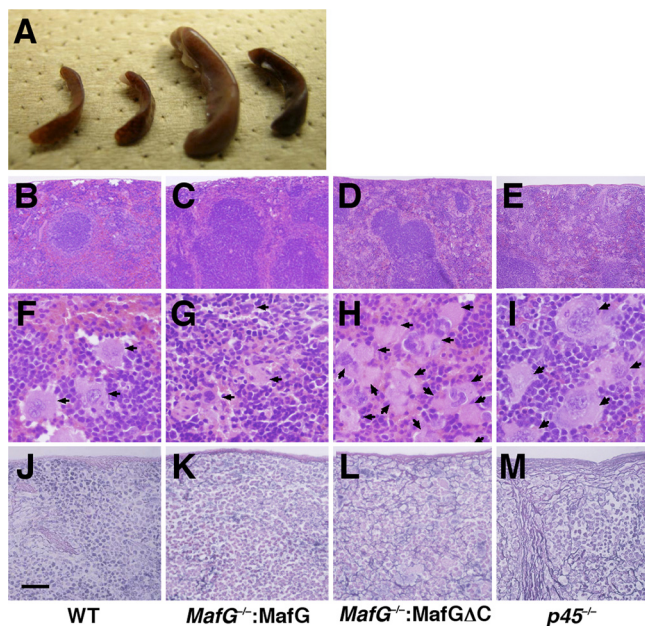
FIG. 5. Accumulation of megakaryocytes and fibrosis observed in spleens of $MafG^{-/-}$::$G1HRD$-MafGΔC mice. (A) Macroscopic observation of spleens. Spleens of (from the left) wild-type, $MafG^{-/-}$::$G1HRD$-MafG line 8, $MafG^{-/-}$::$G1HRD$-MafGΔC line 54, and $MafG^{-/-}$::$G1HRD$-MafGΔC line 36 mice are shown. (B to I) Hematoxylin-and-eosin (HE) staining of spleens of wild-type (B and F), $MafG^{-/-}$::$G1HRD$-MafG line 8 (C and G), $MafG^{-/-}$::$G1HRD$-MafGΔC line 36 (D and H), and $p45$-null (E and I) mice. Arrows indicate megakaryocytes. (J to M) Silver impregnation of spleens of wild-type (J), $MafG^{-/-}$::$G1HRD$-MafG line 8 (K), $MafG^{-/-}$::$G1HRD$-MafGΔC line 36 (L), or $p45$-null (M) mice. Scale bar, 500 μm (B to E), 50 μm (F to I), or 200 μm (J to M).

ciency causes only a modest decrease in platelet number, which is attributed to the compensatory role of MafK, since $MafG$::$MafK$ double mutant mice display severe thrombocytopenia (37). Thus, MafGΔC exerts a dominant-negative activity in a $MafG$-null background. MafGΔC did not affect the red blood cell count (Fig. 4A, lower panel). We also tested whether MafGΔC exerts dominant-negative activity in the wild-type background. Hematological parameters of the three lines of $G1HRD$-MafGΔC mice were assessed. Only line 54, with the highest expression of the transgene, displayed modest but significant thrombocytopenia (Fig. 4B, upper panel), probably because the high level of MafGΔC competitively inhibits abundant MafG as well as MafK expressed in wild-type megakaryocytes. The red blood count was insensitive to MafGΔC (Fig. 4B, lower panel).

As expected from the thrombocytopenia, $MafG^{-/-}$::$G1HRD$-MafGΔC mice displayed splenomegaly (Fig. 5A). Histological examination revealed the abundant accumulation of megakaryocytes in the spleens of $MafG^{-/-}$::$G1HRD$-MafGΔC mice compared with those of wild-type mice and $MafG^{-/-}$::$G1HRD$-MafG mice (Fig. 5B to D and F to H). Fibrosis was evident in the spleens of $MafG^{-/-}$::$G1HRD$-MafΔG mice compared with those of wild-type mice and $MafG^{-/-}$::$G1HRD$-MafG mice (Fig. 5J to L). $MafG^{-/-}$::$G1HRD$-MafGΔC phenotypes resemble those of $p45$-null mice (Fig. 5E,

I, and M)), implying that NF-E2 activity is limiting in $MafG^{-/-}$::MafGΔC mice.

To assess the platelet production capacity of the megakaryocytes, a proplatelet formation (PPF) assay was performed using megakaryocytes isolated from the bone marrow (Fig. 6A). Whereas $MafG$-null megakaryocytes completely lacked PPF ability, megakaryocytes from $MafG^{-/-}$::$G1HRD$-MafG mice generated proplatelets. In contrast, megakaryocytes from $MafG^{-/-}$::$G1HRD$-MafGΔC mice did not. This result also suggested that NF-E2 activity is limiting in $MafG^{-/-}$::$G1HRD$-MafGΔC megakaryocytes.

We examined expression of $Txas$, an established NF-E2 target gene in megakaryocytes (6) (Fig. 6B). $Txas$ expression was reduced in $MafG$-null megakaryocytes, whereas its expression was rescued in $MafG^{-/-}$::$G1HRD$-MafG megakaryocytes. $Txas$ expression was low in $MafG^{-/-}$::$G1HRD$-MafGΔC megakaryocytes, similar to that of $MafG$-null megakaryocytes, indicating that MafGΔC does not confer NF-E2-mediated gene activation.

MafGΔC recruits p45 to the MAREs of $Txas$ and $Nqo1$ promoters. In principle, MafGΔC may not confer NF-E2-dependent transcription due to impairment of p45-MafGΔC heterodimer DNA binding $in vivo$. To investigate this possibility, we used a system in which primary megakaryocytes are cultured from fetal livers. We determined the contribution of MafGΔC to the transcriptional profile in fetal liver-derived megakaryocytes (Fig. 7A). $Txas$ was expressed at a lower level in the primary megakaryocytes from $MafG^{-/-}$::G1HRD-MafGΔC fetal livers than in $MafG^{-/-}$::G1HRD-MafG fetal livers (Fig. 7A, top panel), consistent with the results observed for bone marrow-derived megakaryocytes (Fig. 6B). Expression of an additional NF-E2 target, $Nqo1$ (34), was also lower in MafGΔC-expressing megakaryocytes than in MafG-expressing megakaryocytes (Fig. 7A, bottom panel). Previously, we reported that $solute carrier family 6,$ $member 4$ ($Slc6a4$), $signaling lymphocytic activation molecule$ $family member 1$ ($Slamf1$), P-$selectin$ ($Selp$), and $glycoprotein 6$ ($Gp6$) are direct or indirect p45 targets. Their expression levels were all reduced in MafGΔC-expressing megakaryocytes versus those in MafG-expressing megakaryocytes (Fig. 7A). These results suggest that MafGΔC is incapable of activating transcription as a subunit of NF-E2.

Chromatin immunoprecipitation (ChIP) assays were conducted with primary megakaryocytes cultured from $MafG^{-/-}$::G1HRD-MafG and $MafG^{-/-}$::G1HRD-MafGΔC fetal livers. Chromatin complexes were immunoprecipitated with an anti-p45 antibody (28). In both MafG- and MafGΔC-expressing megakaryocytes, p45 occupied regions containing the $Txas$ MARE and $Nqo1$ MARE but not the $Txas$ intron lacking MAREs (Fig. 7B). In more quantitative assays, p45 occupancy at the $Nqo1$ MARE or $Txas$ MARE was indistinguishable between the two samples (Fig. 7C). Thus, the MafG C terminus is not required for p45 occupancy at MAREs, consistent with our $in vitro$ results demonstrating that the p45-MafGΔC heterodimer binds DNA as strongly as the p45-MafG heterodimer (33).

Since the C-terminal sequence is not required for chromatin occupancy, we asked whether the MafGΔC mutant is defective in specific postchromatin occupancy steps. The enrichment of histone H3 trimethylated at lysine 4 was lower in MafGΔC-
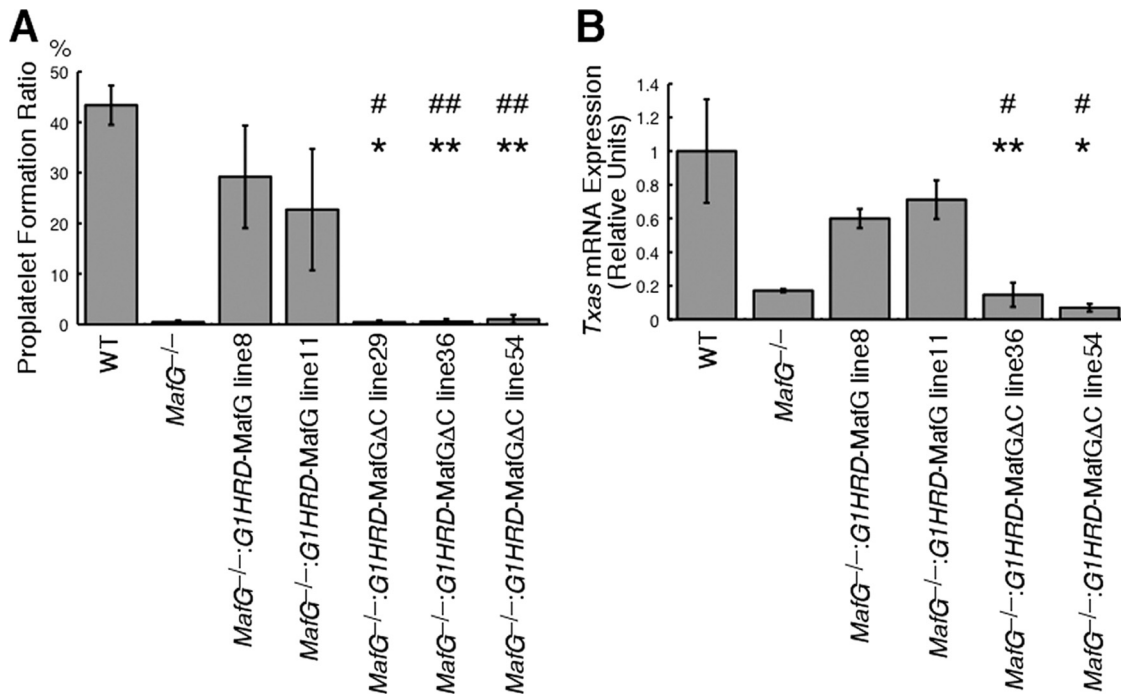
FIG. 6. Defective bone marrow megakaryocytes from $MafG^{-/-}$::$G1HRD$-MafGΔC mice. (A) Proplatelet formation ratios of mature megakaryocytes isolated from bone marrow. Error bars indicate standard deviations of data for more than three mice. GFP-positive megakaryocytes were counted because $G1HRD$-GFP was coinjected with $G1HRD$-MafG or $G1HRD$-MafGΔC so that the transgene expression was monitored at the level of single cells. Student's t test was used to calculate statistical significance (P). ∗ and ∗∗, $P < 0.001$ and $P < 0.01$ compared to values obtained for $MafG^{-/-}$::$G1HRD$-MafG line 8 mice. # and ##, $P < 0.005$ and $P < 0.05$ compared to values obtained for $MafG^{-/-}$::$G1HRD$-MafG line 11 mice. (B) Expression of $Txas$ genes in bone marrow megakaryocytes. The expression level of wild-type cells is set to 1. Error bars indicate standard deviations for triplicate samples. Three independent animals were examined, and the representative result is presented. Student's t test was used to calculate statistical significance (P). ∗ and ∗, $P < 0.002$ and $P < 0.02$ compared to values obtained for $MafG^{-/-}$::$G1HRD$-MafG line 8 mice. #, $P < 0.02$ compared to values obtained for $MafG^{-/-}$::$G1HRD$-MafG line 11 mice.

expressing megakaryocytes than in MafG-expressing mega-karyocytes (Fig. 7C). In contrast, the enrichment of acetylated histone H3 was comparable between the two samples. These results indicate that the MafG C terminus confers maximal H3 trimethylated at K4 and therefore contributes to the establishment of an active chromatin structure, which is consistent with previous reports describing NF-E2-dependent histone H3 methylation at lysine 4 (5, 20).

Considering the presence of a nuclear matrix-targeting signal in the MafG C terminus, we hypothesized that MafG targets NF-E2 to a specific subnuclear compartment, which is necessary to confer proper transcriptional control. We fractionated bone marrow cells of $MafG^{-/-}$::$G1HRD$-MafGΔC mice together with those of wild-type and $MafG$-null mice (Fig. 8A). Compared with wild-type cells, less p45 was retained in the nuclear matrix fraction in $MafG^{-/-}$::$G1HRD$-MafGΔC and $MafG$-null cells. As already shown, a larger amount of MafG associated with the nuclear matrix, while MafGΔC was mostly detected in the soluble nuclear fraction (see Fig. 3C). Interestingly, in $MafG$-null bone marrow cells, the amount of p45 recovered in the cytoplasmic fraction increased, while that in the nuclear and nuclear matrix fractions decreased, implying that MafG facilitates the nuclear localization of p45. These results indicate that the MafG C terminus mediates the association of the p45-MafG heterodimer with the nuclear matrix, which is believed to serve as a scaffold to organize factors

controlling diverse nuclear processes. We propose that MafG functions with p45 to attract and/or stabilize target genes in a specific subnuclear organization, thereby establishing the requisite epigenetic regulation and transcriptional activity.

DISCUSSION

We describe a new mechanism underlying the actions of a critical $trans$-acting factor to control megakaryocyte differentiation and platelet production. Whereas the highly conserved MafG C-terminal sequence was not required for p45 occupancy of chromatin, it was critical to promote NF-E2-mediated target gene regulation. Since this sequence contains a nuclear matrix-targeting signal, we propose that the C-terminal sequence targets NF-E2 to a specific subnuclear compartment, which is necessary to confer proper gene control (Fig. 8B). Intriguingly, the C-terminal sequence activity is critical in the transgenic complementation assay but not in the transient transfection assay with the NF-E2 reporter plasmid. Based on the C-terminal sequence nuclear matrix-targeting activity, which is important in a physiological chromatin context, one would not have expected the activity to be apparent in a transient transfection assay.

MafGΔC exerted a dominant-negative activity on platelet production in $MafG^{-/-}$::$G1HRD$-MafGΔC mice. The platelet count was considerably lower in $MafG^{-/-}$::$G1HRD$-MafGΔC
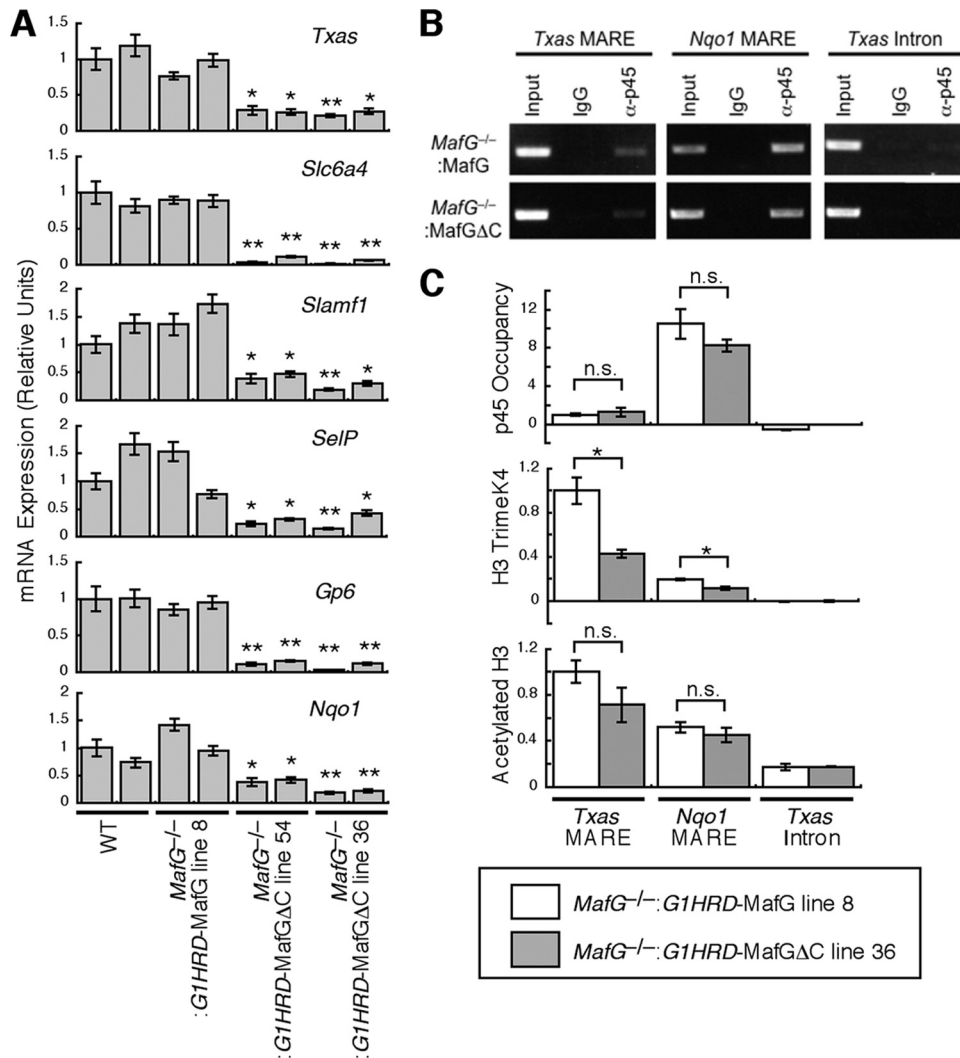
FIG. 7. Recruitment of p45 to the *Txas* promoter in megakaryocytes from $MafG^{-/-}$::*G1HRD*-MafGΔC mice. (A) Expression levels of platelet genes, including *Txas*, in primary megakaryocytes cultured from E14.5 fetal livers. Two independent embryos were examined. The expression levels of the wild-type cells shown in the left bars are set to 1. Error bars indicate standard deviations of data for triplicate samples. Student's *t* test was used to calculate statistical significance (*P*). * and **, $P < 0.005$ and $P < 0.001$ compared to values obtained for wild-type megakaryocytes (shown in the left bar). (B and C) ChIP assay of primary megakaryocytes cultured from E14.5 fetal livers of $MafG^{-/-}$::*G1HRD*-MafG (line 8) mice or $MafG^{-/-}$::*G1HRD*-MafGΔC (line 36) mice using anti-p45 antibody (B and C) and anti-trimethyl-histone H3K4 and anti-acetyl-histone H3 antibodies (C). Enrichment of the promoter regions containing MAREs for the *Txas* and *Nqo1* genes is shown. The third intron of the *Txas* gene was employed as a negative control. Quantitative analysis was performed, and the values represent relative units normalized by input (C). The average values and standard deviations were calculated from triplicate samples. Student's *t* test was used to calculate statistical significance (*P*). * and **, $P < 0.005$ and $P < 0.001$, respectively. n.s., not significant. Two independent experiments were performed, and consistent results were obtained. Representative results are presented.

mice than in *MafG*-null mice (see Fig. 4A), suggesting that MafGΔC inhibits residual activity in *MafG*-null mice. The residual activity may be attributable to MafK, considering that *MafK* deletion in *MafG*-null mice exacerbates thrombocytopenia (37). Thus, we surmise that MafGΔC partially inhibits MafK function in *MafG*-null mice, since *MafG*::*MafK* double mutant mice display considerably more severe thrombocytopenia than $MafG^{-/-}$::*G1HRD*-MafGΔC mice. The platelet count and megakaryocytic gene expression were lower in *G1HRD*-MafGΔC mice from a wild-type background than in wild-type mice (see Fig. 4B; also data not shown), indicating that MafGΔC functions as a dominant-negative mutant in the wild-

type background as well. In contrast, it should be noted that MafGΔC did not exert a dominant-negative effect on erythroid cells (see Fig. 4A and B). Considering this result and our previous report that MafG deficiency has little influence on erythropoiesis (44), erythropoiesis is rather insensitive to reduced NF-E2 activity.

There are two possible interpretations for the dominant-negative activity. The p45-MafGΔC heterodimer might be functionally inactive. Alternatively, the p45-MafGΔC heterodimer might be functional, but the MafGΔC homodimer competitively inhibits p45-MafGΔC heterodimer activity. Because $MafG^{-/-}$::*G1HRD*-MafGΔC line 29 mice express less
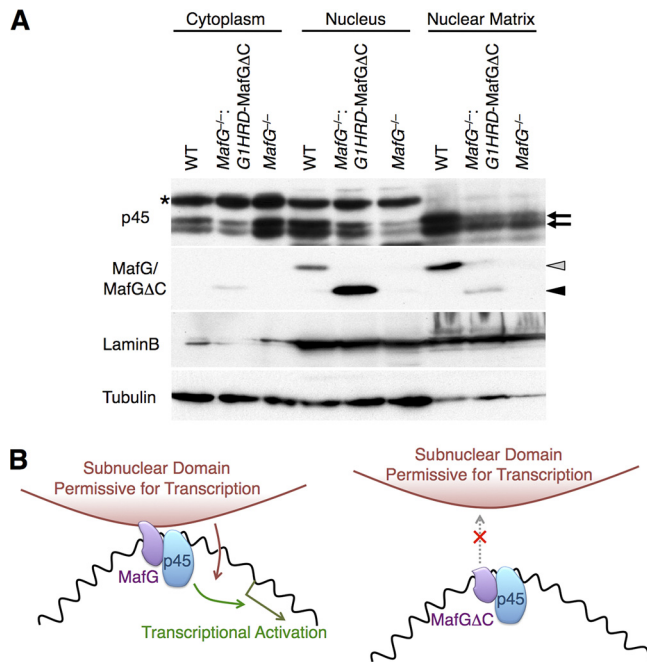
A

B

FIG. 8. Role of MafG in transcriptional activation through determination of subnuclear localization. (A) Fractionation of bone marrow cells from wild-type, *MafG*$^{-/-}$::*G1HRD*-MafGΔC (line 36), and *MafG*-null mice. Lamin B and tubulin were detected as loading controls. Gray and black arrowheads indicate MafG and MafGΔC, respectively, as detected by anti-MafG antibody. Arrows indicate p45. An asterisk indicates nonspecific reactivity of anti-p45 antibody. (B) Model depicting the function of the MafG C terminus. The C terminus of MafG mediates the association of NF-E2 with a specific subnuclear domain and mediates transcriptional activation (left panel). MafGΔC only weakly associates with the subnuclear domain, resulting in the release of p45 into the soluble compartment and impaired transcriptional activation despite normal p45 occupancy of MAREs (right panel). We propose that MafG enhances transcriptional activation by anchoring the p45-MafG heterodimer to the specific subnuclear domain through its C terminus.

MafGΔC than endogenous MafG and phenocopy *p45*-null mice, we favor a model in which the heterodimer is inactive. This interpretation is further supported by the result in which p45 occupied MAREs at target genes similarly in the presence of MafG or MafGΔC. Thus, this work identified a novel function of the MafG C terminus that is necessary for NF-E2 activity.

Chromatin structure and nuclear architecture are important determinants of gene expression (8, 13, 27, 43, 52). The nuclear matrix, biochemically defined as the nuclear structure that persists following the salt extraction of nuclease-treated nuclei, serves as a scaffold for maintaining architectural subnuclear domains and is believed to have an important role in gene expression, replication, and repair (46). Factors involved in transcription (3, 38, 39, 50), RNA processing (51), replication (4), and DNA repair (41) often reside in the nuclear matrix fraction. Whereas the precise functional consequences of the MafG-nuclear matrix association are unclear, it is attractive to consider the notion that MafG-mediated tethering of NF-E2 at the nuclear matrix brings it into the proximity of additional factors necessary for regulation of NF-E2 target genes.

Previous work demonstrated that MafK relocates from the centromeric heterochromatin compartment to the euchromatin compartment upon erythroid differentiation in murine erythroleukemia (MEL) cells (9). This relocation correlates with movement of the β-globin locus away from the nuclear periphery and transcriptional activation of the β-globin gene, a direct target of NF-E2 in cultured erythroid cells. Similarly, during megakaryopoiesis, NF-E2 may use the MafG C terminus to bring the target loci to a specific subnuclear domain, at which gene expression is activated. This is analogous to what has been described for Runx2 (3, 50). Deletion of the Runx2 C terminus simultaneously abrogates its ability to activate transcription and to associate with the nuclear matrix. Analogous to MafG, Runx2 DNA binding activity is unaffected by truncation of the C terminus. Both results highlight the link between locus localization to the requisite nuclear compartment and proper gene control.

MafK and MafG, expressed under the regulation of *G1HRD* in mice, rescue defective megakaryopoiesis in *MafG*-null mice (30). MafF, expressed in hematopoietic cells in mice, seems to rescue thrombocytopenia in compound mutant mice bearing *small Maf* genes (Katsuoka and Yamamoto, unpublished observation). These results enable us to identify the motif responsible within the MafG C terminus as the eight amino acids that are conserved among all small Maf proteins. Because this motif, SVITIVKS, contains a SUMO-interacting motif, which has been defined as Φ-x-Φ-Φ or Φ-Φ-x-Φ, where "Φ" is often V or I (11), sumoylated proteins might associate with the C terminus through the motif. Although no conclusive evidence exists as to whether these eight amino acids are required for association with the nuclear matrix, in principle, MafG may associate with nuclear matrix-associated sumoylated proteins through these eight amino acids, since sumoylated proteins often localize in subnuclear domains that are included in the nuclear matrix fraction (17).

MafG is sumoylated at its N terminus in bone marrow cells (33). There is a well-conserved sumoylation consensus motif in the N-terminal regions of all small Maf proteins. Sumoylation is required for MafG homodimer-mediated repression but antagonizes p45-MafG-mediated transcriptional activation (33). This suggests that sumoylation regulates the conversion of small Maf proteins from transcriptional activators to repressors. Interestingly, MafGΔC expressed in *MafG*-null mice is not sumoylated (data not shown). Thus, the MafG C terminus may be required for association with a SUMO E3 ligase, either directly or indirectly. As the E3 ligase PIASy promotes MafG sumoylation (33) and PIASy localizes to the nuclear matrix (40), MafG may be brought into proximity with PIASy through activity of the C terminus.

In summary, we describe a novel activity residing in the MafG C terminus that mediates association with the nuclear matrix and confers NF-E2-dependent transcriptional activation. This mechanism illustrates a new paradigm in which a specific subunit of a heteromeric *trans*-acting factor complex can confer a specific subnuclear distribution independently of its capacity to promote DNA binding. It will be particularly instructive to assess whether this represents a mechanism common to other bZip heterodimers and more broadly among various types of heterodimeric transcription factors.

REFERENCES

1. **Blencowe, B. J., J. A. Nickerson, R. Issner, S. Penman, and P. A. Sharp.** 1994. Association of nuclear matrix antigens with exon-containing splicing complex. J. Cell Biol. **127:**593–607.
2. **Chen, Z., M. Hu, and R. A. Shivdasani.** 2007. Expression analysis of primary mouse megakaryocyte differentiation and its application in identifying stage-specific molecular markers and a novel transcriptional target of NF-E2. Blood **109:**1451–1459.
3. **Choi, J.-Y., J. Pratap, A. Javed, S. K. Zaidi, L. Xing, E. Balint, S. Dalamangas, B. Boyce, A. J. van Wijnen, J. B. Lian, J. L. Stein, S. N. Jones, and G. S. Stein.** 2001. Subnuclear targeting of Runx/Cbfa/AML factors is essential for tissue-specific differentiation during embryonic development. Proc. Natl. Acad. Sci. U. S. A. **98:**8650–8655.
4. **Dahmcke, C. M., S. Buchmann-Moller, N. A. Jensen, and C. Mitchelmore.** 2008. Altered splicing in exon 8 of the DNA replication factor CIZ1 affects subnuclear distribution and is associated with Alzheimer's disease. Mol. Cell. Neurosci. **38:**589–594.
5. **Demers, C., C.-P. Chaturvedi, J. A. Ranishi, G. Juban, P. Lai, F. Morle, R. Aebersold, F. J. Dilworth, M. Groudine, and M. Brand.** 2007. Activator-mediated recruitment of the MLL2 methyltransferase complex to the β-globin locus. Mol. Cell **27:**573–584.
6. **Deveaux, S., S. Cohen-Kaminsky, R. A. Shivdasani, N. C. Andrews, A. Filipe, I. Kuzniak, S. H. Orkin, P. H. Roméo, and V. Mignotte.** 1997. p45 NF-E2 regulates expression of thromboxane synthase in megakaryocytes. EMBO J. **16:**5654–5661.
7. **Fey, E. G., K. M. Wan, and S. Penman.** 1984. Epithelial cytoskeletal framework and nuclear matrix-intermediate filament scaffold: three dimensional organization and protein composition. J. Cell Biol. **98:**1973–1984.
8. **Francastel, C., D. Schubeler, D. I. Martin, and M. Groudine.** 2000. Nuclear compartmentalization and gene activity. Nat. Rev. Mol. Cell Biol. **1:**137–143.
9. **Francastel, C., W. Magis, and M. Groudine.** 2001. Nuclear relocation of a transactivator subunit precedes target gene activation. Proc. Natl. Acad. Sci. U. S. A. **98:**12120–12125.
10. **Grandori, C., S. M. Cowley, L. P. James, and R. N. Eisenman.** 2000. The Myc/Max/Mad network and the transcriptional control of cell behavior. Annu. Rev. Cell Dev. Biol. **16:**653–699.
11. **Hecker, C.-M., M. Rabiller, K. Haglund, P. Bayer, and I. Dikic.** 2006. Specification of SUMO1- and SUMO2-interacting motifs. J. Biol. Chem. **281:**16117–16127.
12. **Holaska, J. M., and K. L. Wilson.** 2007. An emerin "proteome": purification of distinct emerin-containing complex from Hela cells suggests molecular basis for diverse roles in gene regulation, mRNA splicing, signaling, mechano-sensing and nuclear architecture. Biochemistry **46:**8897–8908.
13. **Hu, Q., Y.-S. Kwon, E. Nunez, M. D. Cardamone, K. R. Hutt, K. A. Ohgi, I. Garcia-Bassets, D. W. Rose, C. K. Glass, M. G. Rosenfeld, and X.-D. Fu.** 2008. Enhancing nuclear receptor-induced transcription requires nuclear motor and LSD1-dependent gene networking in interchromatin granules. Proc. Natl. Acad. Sci. U. S. A. **105:**19199–19204.
14. **Igarashi, K., K. Kataoka, K. Itoh, N. Hayashi, M. Nishizawa, and M. Yamamoto.** 1994. Regulation of transcription by dimerization of erythroid factor NF-E2 p45 with small Maf proteins. Nature **367:**568–572.
15. **Ishii, T., K. Itoh, S. Takahashi, H. Sato, T. Yanagawa, Y. Katoh, S. Bannai, and M. Yamamoto.** 2000. Transcription factor Nrf2 coordinately regulates a group of oxidative stress-inducible genes in macrophages. J. Biol. Chem. **275:**16023–16029.
16. **Itoh, K., T. Chiba, S. Takahashi, T. Ishii, K. Igarashi, Y. Katoh, T. Oyake, N. Hayashi, K. Satoh, I. Hatayama, M. Yamamoto, and Y. Nabeshima.** 1997. An Nrf2/small Maf heterodimer mediates the induction of phase II detoxifying enzyme genes through antioxidant response elements. Biochem. Biophys. Res. Commun. **236:**313–322.
17. **Jackson, P. K.** 2001. A new RING for SUMO: wrestling transcriptional

18. **Katsuoka, F., H. Motohashi, Y. Tamagawa, S. Kure, K. Igarashi, J. D. Engel, and M. Yamamoto.** 2003. Small Maf compound mutants display central nervous system neuronal degeneration, aberrant transcription, and Bach protein mislocalization coincident with myoclonus and abnormal startle response. Mol. Cell. Biol. **23:**1163–1174.
19. **Katsuoka, F., H. Motohashi, T. Ishii, H. Aburatani, J. D. Engel, and M. Yamamoto.** 2005. Genetic evidence that small maf proteins are essential for the activation of antioxidant response element-dependent genes. Mol. Cell. Biol. **25:**8044–8051.
20. **Kiekhaefer, C. M., J. A. Grass, K. D. Johnson, M. E. Boyer, and E. H. Bresnick.** 2002. Hematopoietic-specific activators establish an overlapping pattern of histone acetylation and methylation within a mammalian chromatin domain. Proc. Natl. Acad. Sci. U. S. A. **99:**14309–14314.
21. **Kimura, M., T. Yamamoto, J. Zhang, K. Itoh, M. Kyo, T. Kamiya, H. Aburatani, F. Katsuoka, H. Kurokawa, T. Tanaka, H. Motohashi, and M. Yamamoto.** 2007. Molecular basis distinguishing the DNA binding profile of Nrf2-Maf heterodimer from that of Maf homodimer. J. Biol. Chem. **282:**33681–33690.
22. **Kliewer, S. A., K. Umesono, D. J. Mangelsdorf, and R. M. Evans.** 1992. Retinoid X receptor interacts with nuclear receptors in retinoic acid, thyroid hormone and vitamin D3 signaling. Nature **355:**446–449.
23. **Kyo, M., T. Yamamoto, H. Motohashi, T. Kamiya, T. Kuroita, T. Tanaka, J. D. Engel, B. Kawakami, and M. Yamamoto.** 2004. Evaluation of MafG interaction with Maf recognition element arrays by surface plasmon resonance imaging technique. Genes Cells **9:**153–164.
24. **Lecine, P., J.-L. Villeval, P. Vyas, B. Swencki, Y. Xu, and R. A. Shivdasani.** 1998. Mice lacking transcription factor NF-E2 provide in vivo validation of the proplatelet model of thrombocytopoiesis and show a platelet production defect that is intrinsic to megakaryocytes. Blood **92:**1608–1616.
25. **Levin, J., J.-P. Peng, G. R. Baker, J.-L. Villeval, P. Lecine, S. A. Burstein, and R. A. Shivdasani.** 1999. Pathophysiology of thrombocytopenia and anemia in mice lacking transcription factor NF-E2. Blood **94:**3037–3047.
26. **Massari, M. E., and C. Murre.** 2000. Helix-loop-helix proteins: regulators of transcription in eukaryotic organisms. Mol. Cell. Biol. **20:**429–440.
27. **Misteli, T.** 2007. Beyond the sequence: cellular organization of genome function. Cell **128:**787–800.
28. **Mosser, E. A., J. D. Kasanov, E. C. Forsberg, B. K. Kay, P. A. Ney, and E. H. Bresnick.** 1998. Physical and functional interactions between the transactivation domain of the hematopoietic transcription factor NF-E2 and WW domains. Biochemistry **37:**13686–13695.
29. **Motohashi, H., K. Igarashi, K. Onodera, S. Takahashi, H. Ohtani, M. Nakafuku, M. Nishizawa, J. D. Engel, and M. Yamamoto.** 1996. Mesoder-mal- vs. neuronal-specific expression of MafK is elicited by different promoters. Genes Cells **1:**223–238.
30. **Motohashi, H., F. Katsuoka, J. A. Shavit, J. D. Engel, and M. Yamamoto.** 2000. Positive or negative MARE-dependent transcriptional regulation is determined by the abundance of small Maf proteins. Cell **103:**865–875.
31. **Motohashi, H., T. O'Connor, F. Katsuoka, J. D. Engel, and M. Yamamoto.** 2002. Integration and diversity of the regulatory network composed of Maf and CNC families of transcription factors. Gene **294:**1–12.
32. **Motohashi, H., F. Katsuoka, J. D. Engel, and M. Yamamoto.** 2004. Small Maf proteins serve as transcriptional cofactors for keratinocyte differentiation in the Keap1-Nrf2 regulatory pathway. Proc. Natl. Acad. Sci. U. S. A. **101:**6379–6384.
33. **Motohashi, H., F. Katsuoka, C. Miyoshi, Y. Uchimura, H. Saitoh, C. Francastel, J. D. Engel, and M. Yamamoto.** 2006. MafG sumoylation is required for active transcriptional repression. Mol. Cell. Biol. **26:**4652–4663.
34. **Motohashi, H., M. Kimura, R. Fujita, A. Inoue, X. Pan, M. Takayama, F. Katsuoka, H. Aburatani, E. H. Bresnick, and M. Yamamoto.** 2010. NF-E2 domination over Nrf2 promotes ROS accumulation and megakaryocytic maturation. Blood **115:**677–686.
35. **Nagai, T., K. Igarashi, J. Akasaka, K. Furuyama, H. Fujita, N. Hayashi, M. Yamamoto, and S. Sassa.** 1998. Regulation of NF-E2 activity in erythroleukemia cell differentiation. J. Biol. Chem. **273:**5358–5365.
36. **Onodera, K., J. A. Shavit, H. Motohashi, F. Katsuoka, J. E. Akasaka, J. D. Engel, and M. Yamamoto.** 1999. Characterization of the murine mafF gene. J. Biol. Chem. **274:**21162–21169.
37. **Onodera, K., J. A. Shavit, H. Motohashi, M. Yamamoto, and D. J. Engel.** 2000. Perinatal synthetic lethality and hematopoietic defects in compound mafG::mafK mutant mice. EMBO J. **19:**1335–1345.
38. **Patturajan, M., X. Wei, R. Berezney, and J. L. Corden.** 1998. A nuclear matrix protein interacts with the phosphorylated C-terminal domain of RNA polymerase II. Mol. Cell. Biol. **18:**2406–2415.
39. **Reyes, J. C., C. Muchardt, and M. Yaniv.** 1997. Components of the human SWI/SNF complex are enriched in active chromatin and are associated with the nuclear matrix. J. Cell Biol. **137:**263–274.
40. **Sachdev, S., L. Bruhn, H. Sieber, A. Lichler, F. Melchior, and R. Grosschedl.** 2001. PIASy, a nuclear matrix-associated SUMO E3 ligase, represses LEF1 activity by sequestration into nuclear bodies. Genes Dev. **15:**3088–3103.
41. **Saijo, M., T. Hirai, A. Ogawa, A. Kobayashi, S. Kamiuchi, and K. Tanaka.**

responses into nuclear bodies with PIAS family E3 SUMO ligases. Genes Dev. **15:**3053–3058.

2007. Functionl TFIIH is required for UV-induced translocation of CSA to the nuclear matrix. Mol. Cell. Biol. **27:**2538–2547.

42. **Schmid, M., G. Arib, C. Laemmli, J. Nishikawa, T. Durussel, and U. K. Laemmli.** 2006. Nup-PI: the nucleopore-promoter interaction of genes in yeast. Mol. Cell **21:**379–391.

43. **Schoenfelder, S., T. Sexton, L. Chakalova, N. F. Cope, A. Horton, S. Andrews, S. Kurukuti, J. A. Mitchell, D. Umlauf, D. S. Dimitrova, C. H. Eskiw, Y. Luo, C.-L. Wei, Y. Ruan, J. J. Bieker, and P. Fraser.** 2010. Preferential association between co-regulated genes reveal a transcriptional interactome in erythroid cells. Nat. Genet. **42:**53–62.

44. **Shavit, J. A., H. Motohashi, K. Onodera, J. Akasaka, M. Yamamoto, and J. D. Engel.** 1998. Impaired megakaryopoiesis and behavioral defects in mafG-null mutant mice. Genes Dev. **12:**2164–2174.

45. **Shivdasani, R. A., M. F. Rosenblatt, D. Zucker-Franklin, C. W. Jackson, P. Hunt, C. J. M. Saris, and S. H. Orkin.** 1995. Transcription factor NF-E2 is required for platelet formation independent of the actions of thrombopoietin/MGDF in megakaryocyte development. Cell **81:**695–704.

46. **Stein, G. S., S. K. Zaidi, C. D. Braastad, M. Montecino, A. J. van Wijnen, J.-Y. Choi, J. L. Stein, J. B. Lian, and A. Javed.** 2003. Functional architecture of the nucleus: organizing the regulatory machinery for gene expression, replication and repair. Trends Cell. Biol. **13:**584–592.

47. **Sun, J., H. Hoshino, K. Takaku, O. Nakajima, A. Muto, H. Suzuki, S. Tashiro, S. Takahashi, S. Shibahara, J. Alam, M. M. Taketo, M. Yamamoto, and K. Igarashi.** 2002. Hemoprotein Bach1 regulates enhancer availability of heme oxygenase-1 gene. EMBO J. **21:**5216–5224.

48. **Tiwari, S., J. E. Italiano, Jr., D. C. Barral, E. H. Mules, E. K. Novak, R. T. Swank, M. C. Seabra, and R. A. Shivdasani.** 2003. A role for Rab27b in NF-E2-dependent pathways of platelet formation. Blood **102:**3970–3979.

49. **Yamamoto, T., M. Kyo, T. Kamiya, T. Tanaka, J. D. Engel, H. Motohashi, and M. Yamamoto.** 2006. Predictive base substitution rules that determine the binding and transcriptional specificity of Maf recognition elements. Genes Cells **11:**575–591.

50. **Zaidi, S. K., A. Javed, J.-Y. Choi, A. J. van Wijnen, J. L. Stein, J. B. Lian, and G. S. Stein.** 2001. A specific targeting signal directs Runx2/Cbfa1 to sub-nuclear domains and contributes to transactivation of the osteocalcin gene. J. Cell Sci. **114:**3093–3102.

51. **Zhang, C., D. R. Dowd, A. Staal, C. Gu, J. B. Lian, A. J. van Wijnen, G. S. Stein, and P. N. MacDonald.** 2003. Nuclear coactivator-p62 kDa/Ski-interacting protein is a nuclear matrix-associated coactivator that may couple vitamin D receptor-mediated transcription and RNA splicing. J. Biol. Chem. **278:**35325–35336.

52. **Zhao, R., M. S. Bodnar, and D. L. Spector.** 2009. Nuclear neighborhoods and gene expression. Curr. Opin. Genet. Dev. **19:**172–179.